Identification of potential characteristic genes in chronic skin infections through RNA sequencing and immunohistochemical analysis

HONGYING CAO[1*], WEI XIONG[2*], MEI ZENG[1], LI HU[1], YAN XU[1], WU ZHONG[3] and YINGCHUN HU[1]

[1]Department of Emergency Medicine, The Affiliated Hospital of Southwest Medical University, Luzhou, Sichuan 646000, P.R. China; [2]Department of Emergency Medicine, Leshan People's Hospital, Leshan, Sichuan 614000, P.R. China; [3]Department of Emergency Medicine, Sichuan Provincial Rehabilitation Hospital, Chengdu, Sichuan 611130, P.R. China

Received April 23, 2024; Accepted August 6, 2024

DOI: 10.3892/etm.2024.12721

Abstract. The objective of the present study was to perform RNA sequencing and immunohistochemical analysis on skin specimens obtained from healthy individuals and individuals afflicted with prolonged skin infections. Bioinformatics methodologies were used to scrutinize the RNA sequencing data with the intention of pinpointing distinctive gene signatures associated with chronic skin infections. Skin tissue samples were collected from 11 individuals (4 subjects healthy and 7 patients with chronic skin infections) at the Affiliated Hospital of Southwest Medical University (Luzhou, China). The iDEP tool identified differentially expressed genes (DEGs) with log2 (fold change) ≥2 and q-value ≤0.01. Functional enrichment analysis using Gene Ontology and KEGG databases via the oebiotech online tool was then performed to determine the biological functions and pathways related to these DEGs. A protein-protein interaction network of DEGs identified HIF1A as a potential key gene. Subsequent immunohistochemistry analyses were performed on the samples to assess any variations in HIF1A expression. A total of 900 DEGs, 365 upregulated and 535 downregulated, were observed between the normal and chronic infection groups. The identified DEGs were found to serve a role in various biological processes, including 'hypoxia adaptation', 'angiogenesis', 'cell adhesion' and 'regulation of positive cell migration'. Additionally, these genes were revealed to be involved in the 'TGF-β', 'PI3K-Akt' and 'IL-17' signaling pathways. HIF1A and nine other genes were identified as central nodes in the PPI network. HIF1A expression was higher in chronically infected skin samples than in healthy samples, indicating its potential as a novel research target.

Correspondence to: Professor Wu Zhong, Department of Emergency Medicine, Sichuan Provincial Rehabilitation Hospital, 81 Yongning Street, Wenjiang, Chengdu, Sichuan 611130, P.R. China
E-mail: hongwu2876@sina.com

Professor Yingchun Hu, Department of Emergency Medicine, The Affiliated Hospital of Southwest Medical University, 25 Taiping Street, Jiangyang, Luzhou, Sichuan 646000, P.R. China
E-mail: huyingchun913@swmu.edu.cn.

*Contributed equally

Key words: chronic skin infection, hypoxia-inducible factor 1α, RNA sequencing, immunohistochemistry, bioinformatics

Introduction

Chronic skin infection is caused by bacterial infection, angiogenesis disorders, excessive inflammatory responses and other factors, which in turn cause the deterioration of the skin tissue microenvironment (1). Chronic infection and blood circulation disorders are the main factors that can adversely affect wound healing and the reason that the patient's infectious lesions remain unhealed for a long time (2). Clinically, the treatment of refractory chronic skin infections remains a challenge. Simultaneously, refractory skin infections fail to heal, thereby escalating hospitalization and treatment costs, and consequently augmenting the medical burden on patients. Hypoxia-inducible factor 1α (HIF1A) is commonly found in human cells and is usually expressed under normoxic conditions. However, this protein is quickly broken down by oxygen-dependent ubiquitin proteases within cells and only remains stable at hypoxic conditions. HIF1A can regulate the expression of genes that allow cells to adapt to hypoxic conditions (3-5). RNA sequencing is commonly used to study gene expression and identify new RNAs (6), making it a key tool for analyzing the transcriptome (7). Research on the molecular mechanisms underlying the differences in HIF1A expression between normal tissues and chronically infected skin tissues is required. Based on gene sequencing and bioinformatics analysis of R language data model, differentially expressing genes (DEGs) in tissues from different groups can be screened (8,9). In the present study, skin tissues were collected from healthy human individuals and patients with chronic infection and used for RNA sequencing and immunohistochemical detection. A data model based on R language was used for bioinformatics analysis to find characteristic genes associated with chronic skin infection.

Materials and methods

Sample collection and storage. The present study received approval from the Ethics Committee of the Affiliated Hospital of Southwest Medical University (approval no. KY2022206; Luzhou, China). Prior to participation, all patients (5 males and 2 females; age range, 46-61 years) and volunteers (1 male and 3 females; age range, 37-62 years) provided written informed consent either personally or through their legal representatives. Between May 2022 and May 2023, the Affiliated Hospital of Southwest Medical University gathered seven samples of skin wound tissues from individuals with chronic skin infection, along with four samples of healthy skin tissue from volunteers, which were preserved at -80˚C for RNA sequencing. Additionally, another set of specimens, also comprising four cases in the healthy group and seven cases in the chronic infection group, were washed with pre-cooled PBS and fixed in 4% paraformaldehyde for immunohistochemical detection. Patients with chronic skin infections included post-traumatic infections and diabetic foot infections.

High-throughput mRNA sequencing (RNA-Seq). RNA sequencing was performed on tissue samples from chronic skin infection wounds and healthy individuals using the Illumina Novaseq 6000 sequencing platform (Illumina, Inc.). The Illumina Truseq RNA sample prep Kit (Illumina, Inc.) was used to generate the library and sequence all transcribed mRNA, involving the following six steps: Total RNA extraction; mRNA enrichment with Oligo dT; mRNA fragmentation; cDNA reverse synthesis; adapter ligation; and Illumina sequencing. The specific sequencing process entailed during the extraction was as follows: i) Total RNA from tissue samples, assessment of RNA concentration and purity using Nanodrop 2000 (NanoDrop Technologies; Thermo Fisher Scientific, Inc.), determination of RNA integrity through agarose gel electrophoresis and calculation of RNA integrity number using Agilent 2100 (Agilent Technologies, Inc.); ii) mRNAs were isolated from total RNA by A-T base pairing with polyA using oligo(dT) beads (500 times; cat. no. YH-RCZ-05; Shanghai Majorbio Pharmaceutical Technology Co., Ltd.) to analyze the transcriptomic information, based on the presence of a polyA tail structure at the 3' end of eukaryotic mRNA; iii) the mRNA was fragmented using a fragmentation buffer [DNA Purification and Fragment Screening Kit (magnetic bead method); cat. no. C03-050; Shanghai Meiji Zhuanghua Biopharmaceutical Technology Co., Ltd.], resulting in the isolation of small fragments ~300 bp in length through magnetic bead screening for sequencing; iv) A six-base random primer (random hexamers) is introduced during reverse transcription to generate single-stranded cDNA from mRNA as a template, followed by two-stranded synthesis to establish a stable double-stranded structure; v) end repair mix was added to the double-stranded cDNA structures to homogenize cohesive ends, followed by the addition of an 'A' base at the 3' end for joining Y-shaped joints; vi) the cDNAs obtained through PCR amplifications using Phusion DNA polymerase (NEB) for 15 cycles according to the manufacturer's instructions; recovered with 2% agarose gel, quantified using TBS380 (PicoGreen; NovaSeq Reagent Kit; Illumina, Inc.) and run in a data ratio; and vii) bridge PCR was then amplified on cBot to generate clusters, which were subsequently sequenced on the Illumina platform (Illumina, Inc.) using a PE library with a reading length of 2x150 bp.

Screening for DEGs. The sequencing data, which were subjected to quality control measures [log2(CPM+4)], were analyzed using the online software idep.96 (http://bioinformatics.sdstate.edu/idep/) (10) and a network tool (http://bioinformatics.sdstate.edu/idep/) based on the R language (http://www.R-project.org/). Data quality was standardized by applying $\log_2$ (CPM)+4 (11), before the DESeq2 differential screening method [$\log_2$ fold-change (FC)≥1 and q-value ≤0.05] (12) was used to identify DEGs between the healthy skin group and the chronically infected skin group.

Gene ontology (GO) and Kyoto Encyclopedia of Genes and Genomes (KEGG) functional enrichment analysis. GO analysis is a typical batch gene data analysis method. The GO examination of genes involved the analysis of biological process (BP), cellular component (CC) and molecular function (MF) aspects, was performed for categorizing and identifying groups of genes in subsequent stages (13). KEGG is a resource that systematically examines gene signaling pathways and connects genomic and functional data (14). The chosen DEGs were assessed using the database to study GO functions and KEGG pathways, with the results being visualized through online tools utilizing R language (https://cloud.oebiotech.com/spa#/bio/detail?number=e267d1a2-4303-44d7-a6db-d2bd2ad59e3e).

Protein-protein interaction (PPI) analysis. Core genes were identified through the construction of a PPI network utilizing the STRING database (https://cn.string-db.org/) (15) to understand how genes interacted at the protein level. Potential key targets were identified through this analysis. DEGs were then filtered based on their node degree and network, with a threshold comprehensive score of >0.4. The present study focused on the functional interactions among target genes and other genes associated with adapting to hypoxia, angiogenesis, cell adhesion and cell migration.

Immunohistochemistry. The present study adhered to the typical protocols of immunohistochemistry, including collecting materials, preparing sections, conducting antigen-antibody reactions and developing colors to identify the presence of HIF1A expression in healthy skin samples from donors and in wound tissues from patients with chronic skin infections. The specific procedures for immunohistochemistry were as follows: i) Skin tissues were fixed in 4% paraformaldehyde, embedded in paraffin wax and cut into 5-mm slices. The slices were then pressed onto anti-slip plates and placed on a 60˚C microtome for 2 h. ii) The sections were incubated twice in xylene and dehydrated in gradient ethanol solutions. iii) After microwave treatment in citrate buffer (pH 6.0), the slides were incubated in 3% hydrogen peroxide for 15 min to inhibit endogenous peroxidase activity. They were then blocked with 10% normal goat serum (cat. no. A0208; Beyotime Institute of Biotechnology) and incubated at room temperature for 10 min. iv) Sections were treated with primary antibodies (HIF-1α polyclonal antibody; 1:70; cat. no. 20960-1-AP; Proteintech

Group, Inc.) as per instructions and incubated overnight at 4˚C. After rewarming for 30 min at room temperature, they were incubated with HRP-labeled secondary antibody [HRP-labeled goat anti-rabbit IgG (HL); 1:70; cat. no. A0208; Beyotime Institute of Biotechnology) for 60 min. Specimens were then washed three times in PBS for 5 min each. v) Sections were colored with DAB for 1-10 min, then washed twice in distilled water for 5 min each. Hematoxylin counterstaining was performed for 5 min, followed by dehydration with gradient alcohol and clearing with xylene twice for 5 min each. A neutral gummy film was applied for capturing images. Images were viewed using an inverted light microscope and captured at a magnification of x100 and x200. ImageJ (version 1.8.0_172) processing software (National Institutes of Health) was used for the semi-quantitative analysis of immunohistochemical staining and to determine the average optical density (AOD) value.

Statistical analysis. Statistical analysis of experimental data was conducted using SPSS 26.0 software (IBM Corp). The experimental results consist of measurements that follow a normal distribution and are represented by the mean ± standard deviation. Unpaired t-tests were used for comparing between the two means.

Results

Quality control of genetic data obtained from sequencing. The gene data set obtained through RNA-seq underwent logarithmic processing and was subjected to quality control using the online analysis software idep.96 (http://bioinformatics.sdstate.edu/idep/), which primarily involved generating box plots for two datasets (Fig. 1), data density plot (Fig. 2) and principal component analysis plot (Fig. 3). The analysis results indicated that the data were comparable and the quality control of the data was satisfactory.

Differential gene screening. After the initial dataset was preprocessed using logarithmic transformation, it was analyzed using the online tool idep 0.96 (http://bioinformatics.sdstate.edu/idep/) with the criteria of FC>4 and P<0.05. In both the chronic infection group and healthy group, 900 DEGs were found, with 365 genes being upregulated and 565 genes being downregulated. The DEGs were found to be evenly distributed between the groups. The details of DEGs are shown in the bar chart (Fig. 4) and volcano chart (Fig. 5).

Enrichment analysis of differential genes. After screening the 900 DEGs, an analysis was conducted on their GO functions and KEGG pathways using a database, before the results were visualized with the R language-based oebiotech online tool. The examination revealed that the DEGs primarily participate in biological activities such as 'response to hypoxia', 'angiogenesis' and 'cell adhesion' (Fig. 6). Additionally, they served a role in various signaling pathways, including TGF-β, PI3K-Akt and IL-17 (Fig. 7).

PPI network. A total of 1,104 DEGs were used to create the PPI network. From this network, 10 genes were identified as being central to the network, involved in various biological processes

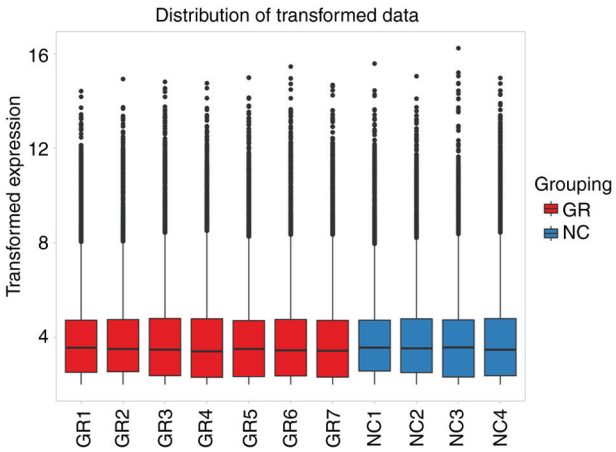

Figure 1. Box plots. In the figure, the abscissa denotes the sample (distribution of transformed data), whilst the ordinate represents the gene expression value post logarithmic transformation (transformed expression). The rectangular bars correspond to the individual samples, with blue denoting the healthy skin group and red representing the chronic skin infection group. The black line within each rectangle signifies the average gene expression value of the respective sample. The proximity of the average logarithmic gene expression values across all samples suggests comparability and indicates satisfactory data quality control. NC, healthy skin group; GR, chronic skin infection group.

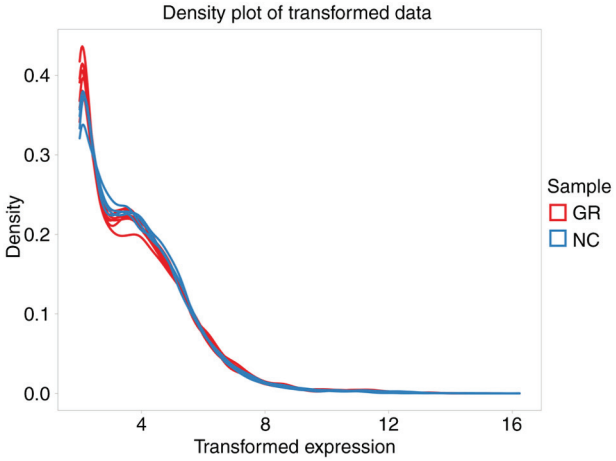

Figure 2. Data density chart. On the graph, the x-axis shows the expression value (transformed expression) and the y-axis indicates the data density (density plot of transformed data). The blue color signifies the healthy skin group of the donor, whereas the red color represents the chronic skin infection group. The graph shows distinct densities between the red and blue lines, revealing a significant contrast in expression values between the two data sets, implying effective data quality management. NC, healthy skin group; GR, chronic skin infection group.

such as angiogenesis, protein modification, intracellular signal transduction, cell biosynthetic processes, catabolism regulation, organ morphogenesis and movement regulation (Fig. 8).

Immunohistochemistry. Healthy skin tissues exhibit distinct layers, such as the epidermis, containing the stratum corneum, stratum lucidum, stratum granulosum, stratum spinosum and basal cell sublayers, in addition to the dermis with its papillary and reticular layers. Immunohistochemistry was conducted on samples obtained from four individuals in the healthy skin group and seven individuals in the chronic skin infection

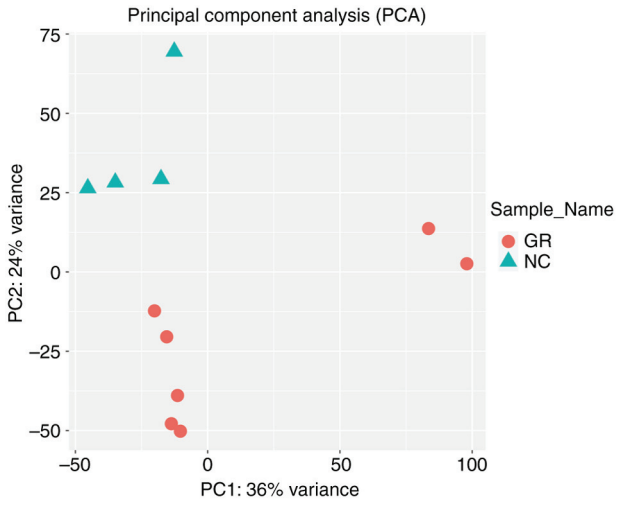

Figure 3. Principle component analysis plot. The x-axis in the given diagram corresponds to the initial principal component PC1, and the y-axis represents the second principal component PC2. Each data point in the plot signifies a distinct sample, with varying groups distinguished by different colors (red denoting the chronic skin infection group and blue representing the normal skin of volunteers group). The figure demonstrates clear differentiation between the two groups. PC, principle component. NC, healthy skin group; GR, chronic skin infection group.

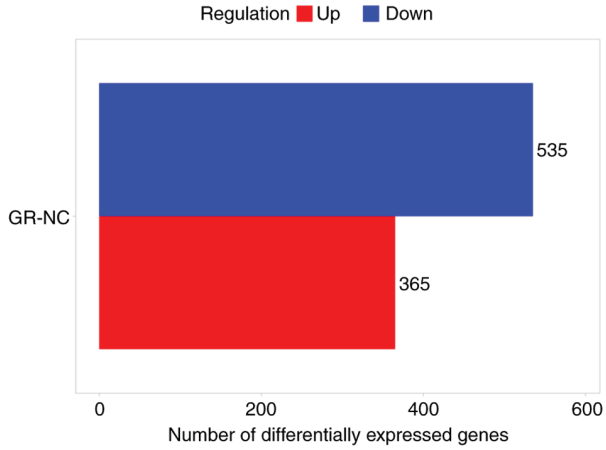

Figure 4. DEGs bar chart. The x-axis indicates the quantity of genes, with red indicating the quantity of genes that are upregulated and blue indicating the quantity of genes that are downregulated. Comparing the chronic infection group with the healthy group, 900 DEGs were found, including 365 upregulated genes and 535 downregulated genes. DEGs, differentially expressing genes. NC, healthy skin group; GR, chronic skin infection group.

group to assess the presence of HIF1A expression. In the chronic infection group, observations revealed thickening of the epidermal cuticle, destruction of the basal layer, proliferation of fibrous tissue and disorganized arrangement of muscle fibers. Analysis indicated the expression of HIF1A in the dermis. Semi-quantitative analysis of HIF1A was performed using ImageJ (version 1.8.0_172) software (National Institutes of Health) to determine the AOD value as a measure of HIF1A expression. The mean ± standard deviation was used to describe the experimental data. The healthy group had an AOD value of 0.207828±0.007539, whilst the chronic infection group had a value of 0.221970±0.009962. The data from the experiment followed a normal distribution. A comparison between groups was conducted using an unpaired t-test, revealing a statistical difference ($P<0.05$; Fig. 9). These findings suggest that HIF1A was highly expressed in the chronic infection group.

Discussion

Chronic infections in the skin typically exhibit persistent inflammation, posing challenges for effective healing (16). Hypoxia has been previously identified as a contributing factor to the aggravation of chronically infected skin tissues (17). The body response to hypoxia involves the stimulation of angiogenesis, increasing blood flow and enhanced oxygenation (18). A prior study revealed that in low-oxygen conditions, endothelial cells are key in starting angiogenesis by accumulating HIF1A to address hypoxia (19). Hypoxia serves as the primary stimulus for the upregulation of HIF1A expression, which in turn serves a crucial role in orchestrating the cellular response to hypoxia (20,21). The expression of HIF1A is typically elevated under hypoxic conditions, where it is involved in various processes, such as angiogenesis and cell metabolism (18).

For the present study, specimens were collected from individuals with diabetic skin infection, traumatic skin infection and other chronic skin infections for analysis using immunohistochemistry, RNA-seq and bioinformatics techniques. Immunohistochemical analysis revealed the increased expression of HIF1A in chronically infected skin tissues. Furthermore, RNA-seq identified upregulated expression of the HIF1A gene in blood samples from individuals with chronic skin infections. Bioinformatics analysis revealed that the DEGs primarily implicated in the PI3K-Akt, TGF-β and IL-17 signaling pathways.

Skin infections in patients with diabetes present a challenge in wound healing due to the effects of high blood sugar on the microvascular basement membrane and endothelial cells, resulting in chronic ischemia and hypoxia of the tissue (22). Additionally, the formation of chronic infection wounds in the skin tissue can lead to vascularization disorders and hindered epithelialization (23). Fridoni *et al* (24) previously reported an increase in HIF1A expression in the infected wound tissue of diabetic rats. This phenomenon may be attributed to the significant enhancement of HIF1A expression by human bone marrow cell MSC-EV, leading to the transformation of macrophages from the M1 to the M2 phenotype. Guo *et al* (25) and Jiang *et al* (26) previously demonstrated that increased HIF1A expression can facilitate skin wound vascularization and accelerate the healing process of diabetic foot ulcers by upregulating VEGF expression, suppressing inflammation, promoting angiogenesis, and facilitating skin ulcer healing. In a study by Liu *et al* (27), it was observed that HIF1A exhibited decreased expression levels in skin tissues affected by diabetic wounds. Similarly, Liu *et al* (27) reported a significant reduction in HIF1A expression in biopsy samples from individuals with diabetic foot infections. These findings indicate a potential association between diminished HIF1A levels and inadequate angiogenic factors, suggesting that reduced HIF1A expression can serve a pivotal role in the delayed healing of wounds (28).

Angiogenesis serves an important role in the repair of chronically infected skin wounds, by facilitating the formation of new blood vessels that supply oxygen and nutrients

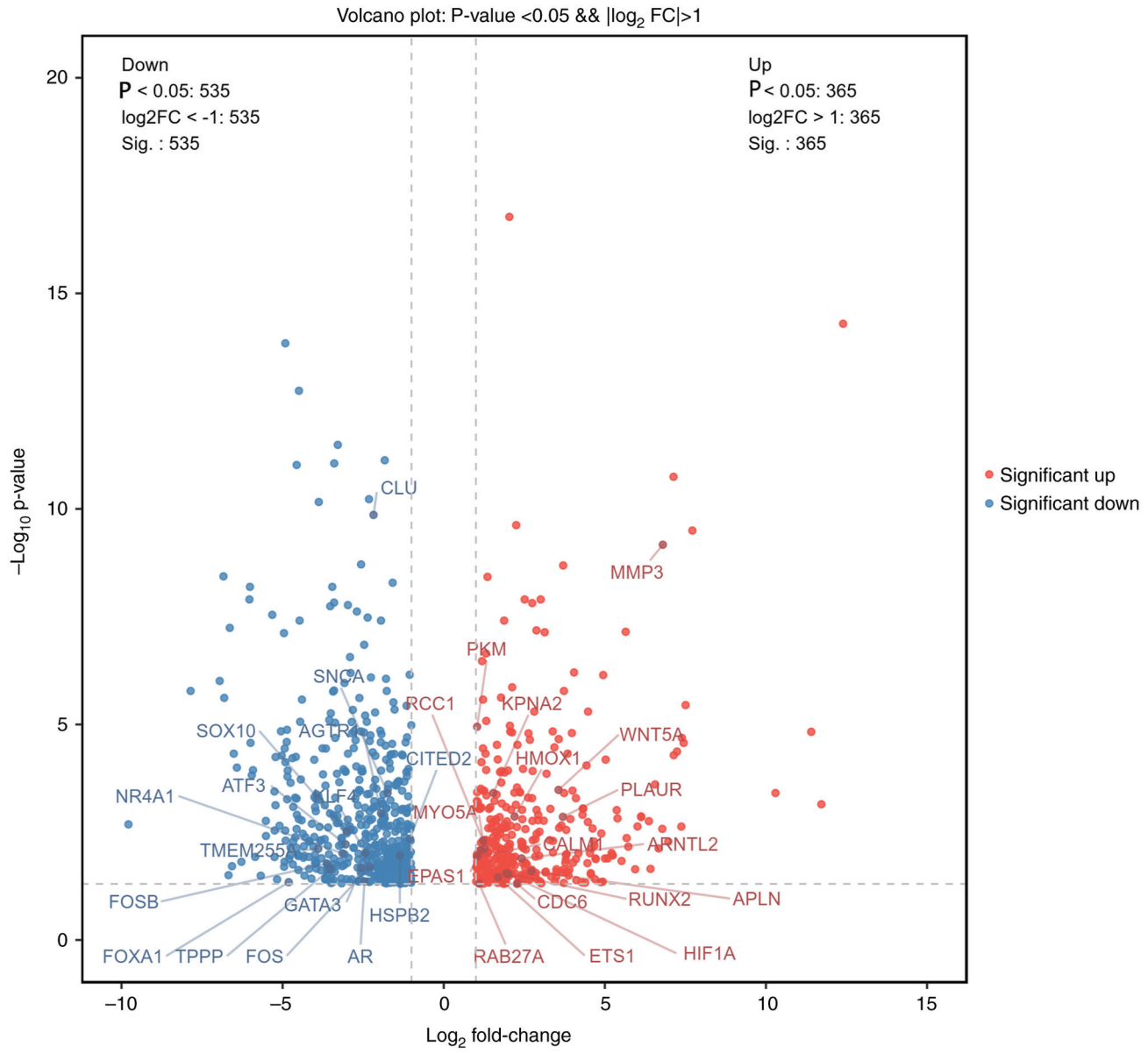

Figure 5. Volcano diagram. The vertical axis displays the logarithmic false discovery rate expression value for genes that are DEGs, with the horizontal axis showing the logarithmic fold change in biological repeats for the DEGs. The color red indicates upregulation, while blue indicates downregulation. A total of 900 DEGs were identified in both the healthy and chronic infection groups, with 365 being upregulated and 535 being downregulated. DEGs, differentially expressing genes; NC, healthy skin group; GR, chronic skin infection group.

necessary for tissue regeneration (29). The PI3K/AKT cell signaling pathway, known for its involvement in various cellular functions, such as proliferation, autophagy, senescence and apoptosis, may be activated by the hypoxia-induced upregulation of HIF1A during this process (30-32). It has been previously demonstrated that activation of the PI3K/AKT/mTOR pathway can enhance VEGF expression by upregulating HIF1A to promote angiogenesis (33). It is becoming accepted that VEGF is a key angiogenic factor among the various well-known pro-angiogenic factors (34). Activation of the PI3K/AKT signaling pathway has been shown to result in the upregulation of HIF1A and increased VEGF expression, subsequently facilitating the development of new blood vessels. Inhibiting the VEGF signaling pathway is hypothesized to suppress angiogenesis (35). The present study used RNA-seq and bioinformatics techniques, followed by enrichment analysis of the identified DEGs, to reveal the enrichment of genes in the PI3K/AKT signaling pathway.

Previous studies have demonstrated that the HIF1A/VEGF signaling pathway can serve a crucial role in mediating the skin wound healing process by regulating a number of key biological processes, including inflammation, angiogenesis, fibroblast proliferation and re-epithelialization (36). The present study also found that HIF1A expression was different between the chronic infected skin and healthy skin. Gene detection and immunohistochemistry analysis in the chronic infection group revealed the high expression of HIF1A, suggesting its potential role as a pivotal gene in the repair process of chronically infected skin tissue. Furthermore, functional enrichment analysis of DEGs in the chronic infection group compared with the healthy group suggests that HIF1A may be associated with the PI3K/AKT signaling pathway, which can potentially

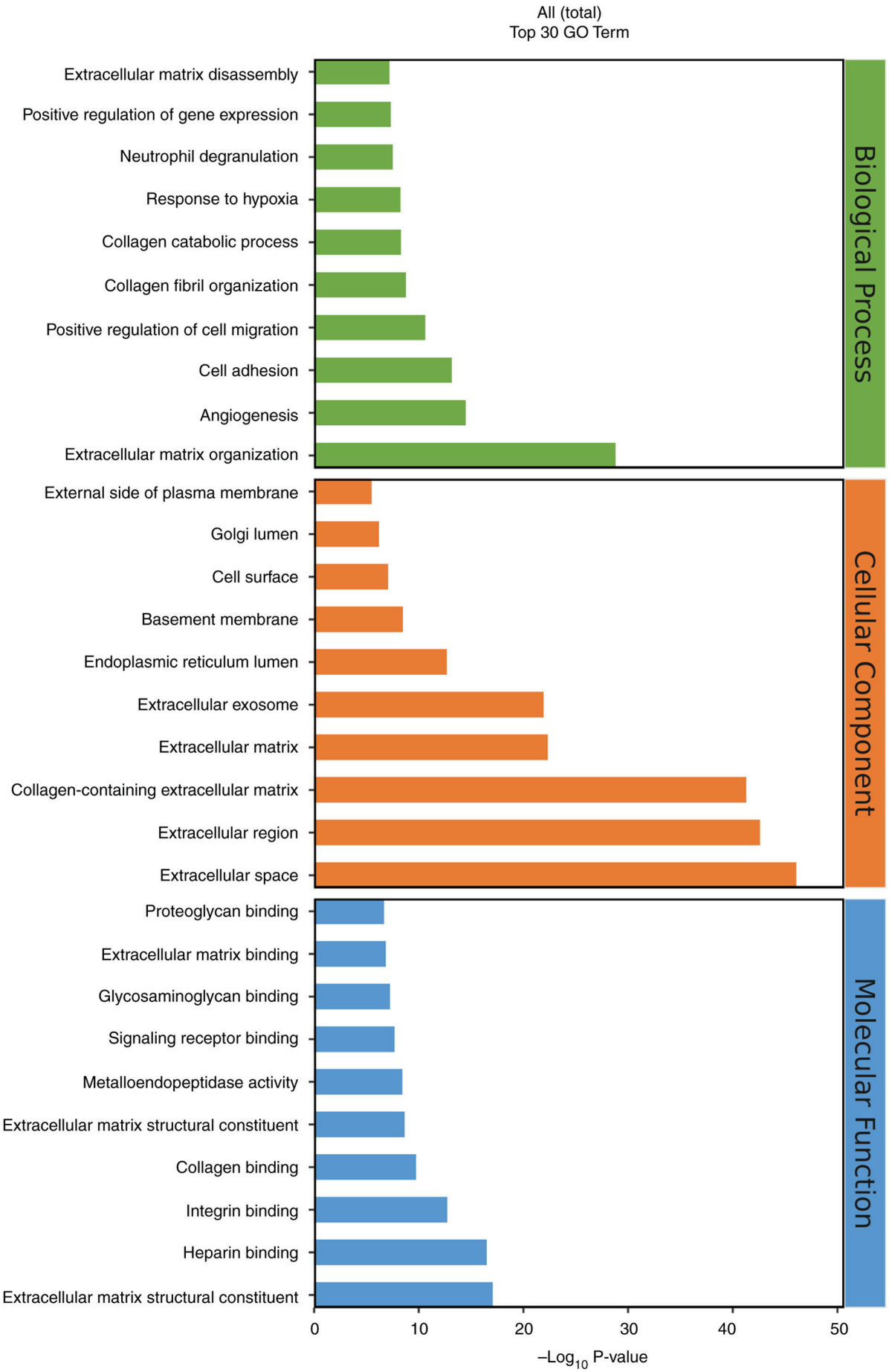

Figure 6. GO enrichment analysis diagram. The horizontal axis denotes the enrichment factor and the vertical axis denotes the enrichment outcomes of the top 30 biological processes. Enrichment analyses encompassed biological processes, cellular components and molecular functions. GO, gene ontology.

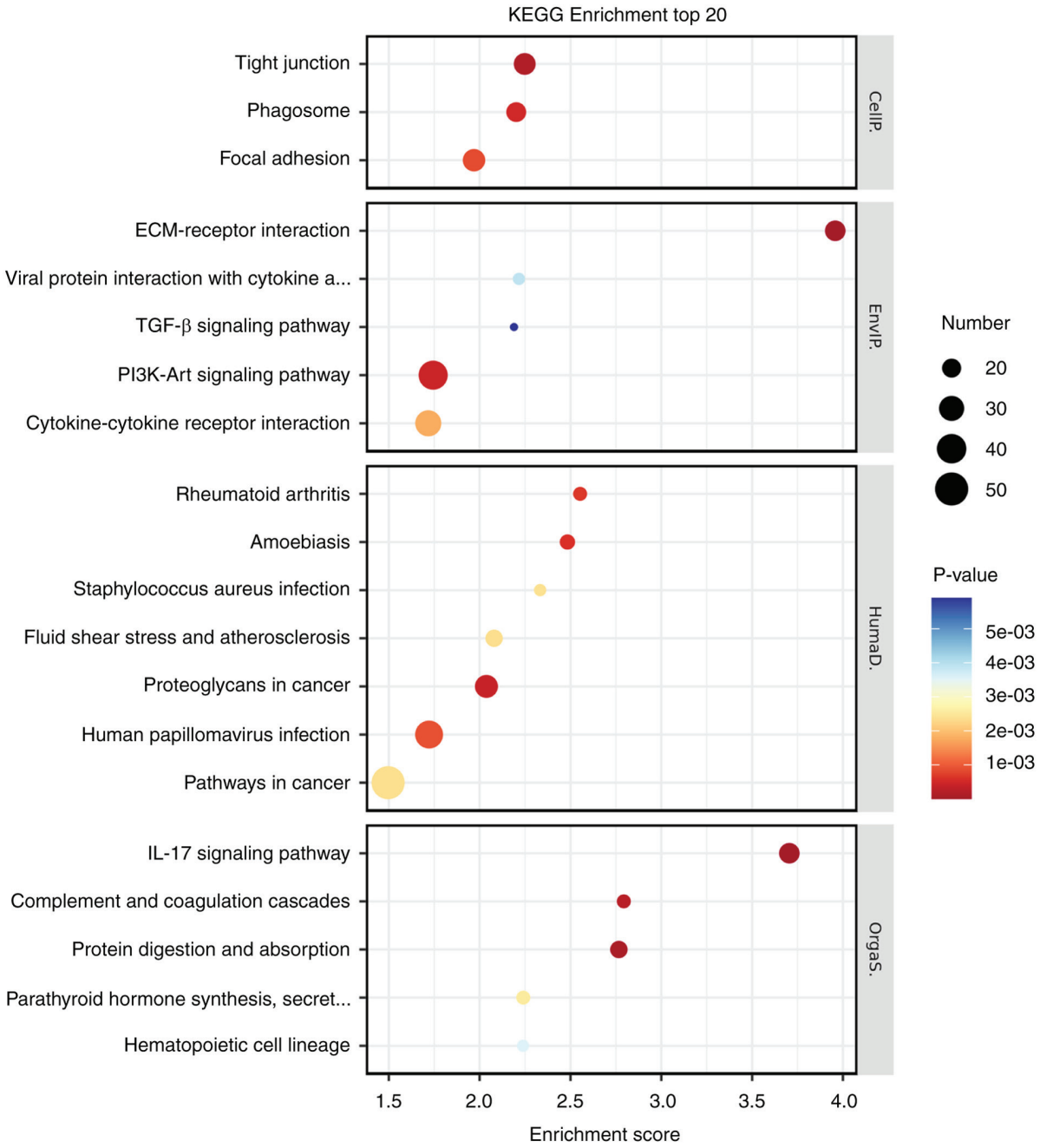

Figure 7. KEGG pathway enrichment analysis diagram. The horizontal axis (enrichment score) signifies the enrichment factor, whilst the vertical axis (KEGG enrichment top 20) represents the top 20 signaling pathways involving differentially expressed genes. The size of the data points in the graph corresponds to the number of enriched genes in the biological process, whilst the variation in color indicates the significance level of the P-value. KEGG, Kyoto Encyclopedia or Genes and Genomes.

contribute to the healing process of chronic infected skin wounds through a yet unidentified mechanism.

Nevertheless, it is important to acknowledge the limitations of the present study. The small sample size may have restricted the ability to fully explore the phenomenon and uncover potential mechanisms. Additionally, the present study did not definitively establish HIF1A as the target gene for chronic infected skin wound repair, where its underlying mechanism remains unclear. Future studies may benefit from expanding the sample size. It is also imperative to investigate the expression levels of HIF1A and pathways associated with angiogenesis and downstream cytokines in tissues of chronic skin infection wounds. The present study research suggested that HIF1A may serve a role in the healing of chronic infected skin wounds by modulating various processes, such as inflammation and angiogenesis. Additionally, the present study identified a potential association between HIF1A and the PI3K/AKT signaling pathway. Future studies may involve the detection of inflammatory factors, vascular markers and other relevant molecules.

To conclude, the present study identified a significant upregulation of HIF1A in chronically infected skin tissue, suggesting its potential role as a pivotal gene in the reparative mechanisms associated with chronic skin infections.

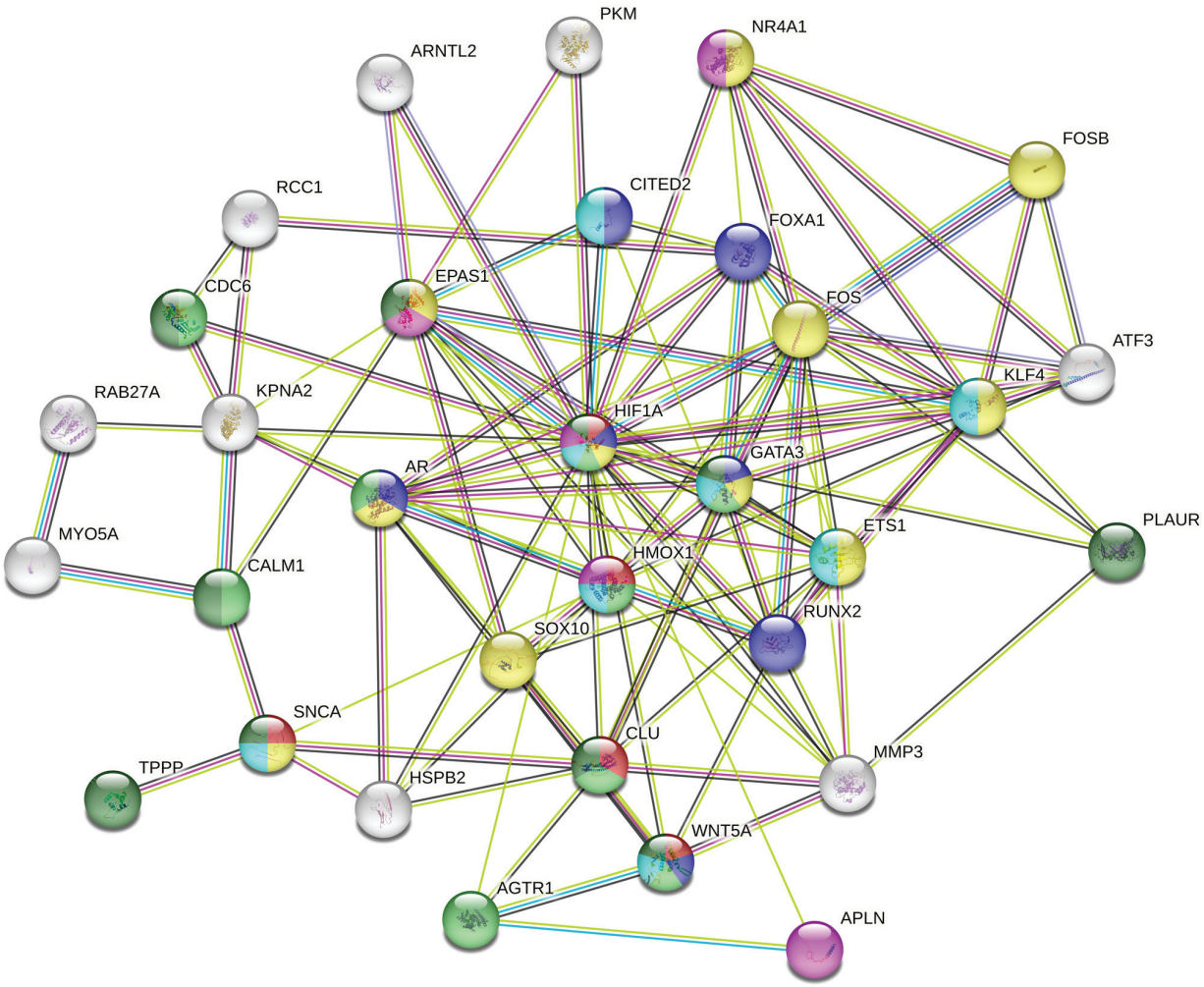

Figure 8. PPI network analysis diagram. Each dot symbolizes a gene, including 10 core genes (*HIF1A*, *GATA3*, *HMOX1*, *ETS1*, *AR*, *CLU*, *RUNX2*, *AR*, *KLF* and *CDC6*) situated centrally within the PPI network. PPI, protein-protein interaction.

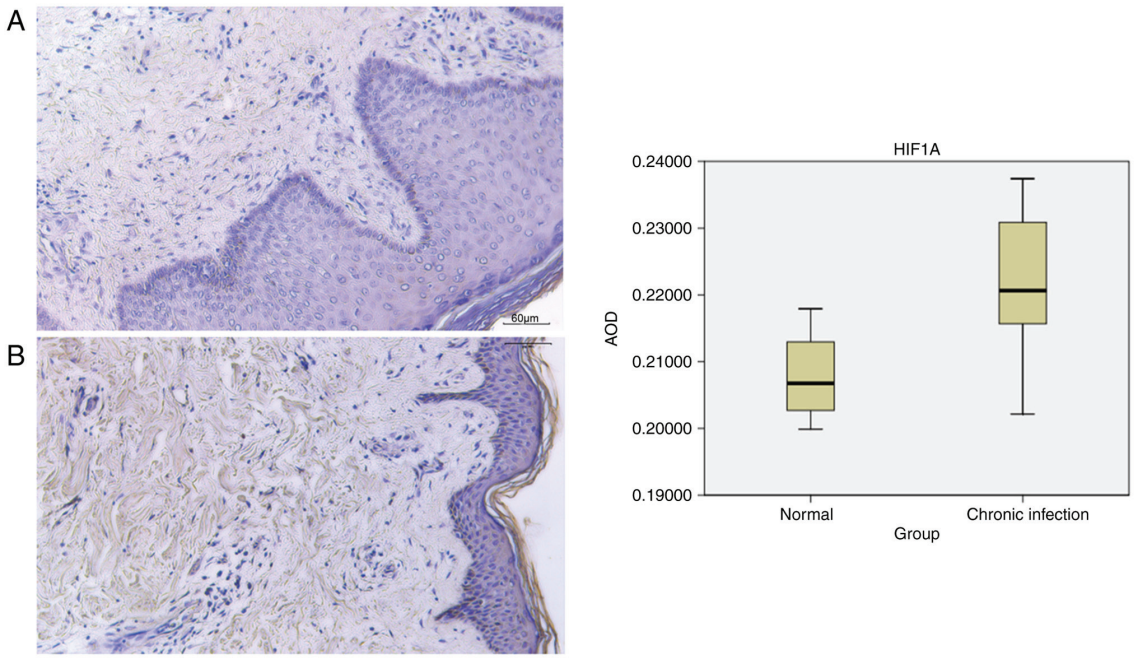

Figure 9. Immunohistochemistry. ImageJ software was used to semi-quantitatively analyze the AOD value. SPSS software was then used to analyze and compare the expression values of HIF1A between the healthy group and the chronic infection group. P<0.05. Immunohistochemical staining of HIF1A in (A) the normal group and (B) the chronic infection group. AOD, average optical density; HIF1A, hypoxia-inducible factor 1A.

Furthermore, HIF1A may be involved in the PI3K/AKT signaling pathway. These findings offer a foundation for future investigations into potential biological targets for the treatment of chronic skin infections.

Acknowledgements

Not applicable.

Funding

The present study was supported by the Southwest Medical University (grant no. 0903-00031431).

Availability of data and materials

The data generated in the present study may be found in the China National GeneBank DataBase under accession number (CNP0004833) or at the following URL: http://db.cngb.org/cnsa/project/CNP0004833_09297f74/reviewlink/. Other data generated in the present study may be requested from the corresponding author.

Authors' contributions

YCH and WZ designed the study. HYC, WX, MZ, LH and YX performed the experiments. HYC and WX acquired and analyzed the data. MZ applied for clinical ethics approval and obtained the clinical samples. LH and YX obtained the clinical samples. HYC wrote and revised the manuscript. YCH and WZ confirm the authenticity of all the raw data. All authors read and approved the final version of the manuscript.

Ethics approval and consent to participate

All methods were conducted in compliance with all applicable rules and regulations. The peripheral blood and skin tissue samples were acquired from patients who were hospitalized in the Affiliated Hospital of Southwest Medical University (Luzhou, China). All experiments were authorized by the hospital's ethics committee (approval no. KY2022206) and conformed to the Declaration Helsinki guidelines. Written informed consent was obtained from all subjects.

Patient consent for publication

Not applicable.

Competing interests

The authors declare that they have no competing interests.

References

1. Jull AB, Cullum N, Dumville JC, Westby MJ, Deshpande S and Walker N: Honey as a topical treatment for wounds. Cochrane Database Syst Rev 2015: CD005083, 2015.
2. Wen Q, Liu D, Wang X, Zhang Y, Fang S, Qiu X and Chen Q: A systematic review of ozone therapy for treating chronically refractory wounds and ulcers. Int Wound J 19: 853-870, 2022.
3. Wenger RH, Stiehl DP and Camenisch G: Integration of oxygen signaling at the consensus HRE. Sci STKE 2005: re12, 2005.
4. Semenza GL: Oxygen-dependent regulation of mitochondrial respiration by hypoxia-inducible factor 1. Biochem J 405: 1-9, 2007.
5. Iyer NV, Kotch LE, Agani F, Leung SW, Laughner E, Wenger RH, Gassmann M, Gearhart JD, Lawler AM, Yu AY and Semenza GL: Cellular and developmental control of O2 homeostasis by hypoxia-inducible factor 1 alpha. Genes Dev 12: 149-162, 1998.
6. Hrdlickova R, Toloue M and Tian B: RNA-Seq methods for transcriptome analysis. Wiley Interdiscip Rev RNA 8: 10.1002/wrna.1364, 2017.
7. Shi H, Zhou Y, Jia E, Pan M, Bai Y and Ge Q: Bias in RNA-seq library preparation: Current challenges and solutions. Biomed Res Int 2021: 6647597, 2021.
8. Andrews TS, Kiselev VY, McCarthy D and Hemberg M: Tutorial: Guidelines for the computational analysis of single-cell RNA sequencing data. Nat Protoc 16: 1-9, 2021.
9. Lafzi A, Moutinho C, Picelli S and Heyn H: Tutorial: Guidelines for the experimental design of single-cell RNA sequencing studies. Nat Protoc 13: 2742-2757, 2018.
10. Ge SX, Son EW and Yao R: iDEP: An integrated web application for differential expression and pathway analysis of RNA-Seq data. BMC Bioinformatics 19: 534, 2018.
11. Robinson MD, McCarthy DJ and Smyth GK: edgeR: A Bioconductor package for differential expression analysis of digital gene expression data. Bioinformatics 26: 139-140, 2010.
12. Love MI, Huber W and Anders S: Moderated estimation of fold change and dispersion for RNA-seq data with DESeq2. Genome Biol 15: 550, 2014.
13. Ge SX, Jung D and Yao R: ShinyGO: A graphical gene-set enrichment tool for animals and plants. Bioinformatics 36: 2628-2629, 2020.
14. Ge X: iDEP Web application for RNA-Seq data analysis. Methods Mol Biol 2284: 417-443, 2021.
15. Szklarczyk D, Gable AL, Nastou KC, Lyon D, Kirsch R, Pyysalo S, Doncheva NT, Legeay M, Fang T, Bork P, *et al*: Correction to 'The STRING database in 2021: Customizable protein-protein networks, and functional characterization of user-uploaded gene/measurement sets'. Nucleic Acids Res 49: 10800, 2021.
16. Martin P: Wound healing-aiming for perfect skin regeneration. Science 276: 75-81, 1997.
17. Tandara AA and Mustoe TA: Oxygen in wound healing-more than a nutrient. World J Surg 28: 294-300, 2004.
18. Fong GH: Mechanisms of adaptive angiogenesis to tissue hypoxia. Angiogenesis 11: 121-140, 2008.
19. Cash TP, Pan Y and Simon MC: Reactive oxygen species and cellular oxygen sensing. Free Radic Biol Med 43: 1219-1225, 2007.
20. Pawar KB, Desai S, Bhonde RR, Bhole RP and Deshmukh AA: Wound with diabetes: Present scenario and future. Curr Diabetes Rev 17: 136-142, 2021.
21. Salazar JJ, Ennis WJ and Koh TJ: Diabetes medications: Impact on inflammation and wound healing. J Diabetes Complications 30: 746-752, 2016.
22. Thangarajah H, Yao D, Chang EI, Shi Y, Jazayeri L, Vial IN, Galiano RD, Du XL, Grogan R, Galvez MG, *et al*: The molecular basis for impaired hypoxia-induced VEGF expression in diabetic tissues. Proc Natl Acad Sci USA 106: 13505-13510, 2009.
23. Wang X, Li R and Zhao H: Enhancing angiogenesis: Innovative drug delivery systems to facilitate diabetic wound healing. Biomed Pharmacother 170: 116035, 2024.
24. Fridoni M, Kouhkheil R, Abdollhifar MA, Amini A, Ghatrehsamani M, Ghoreishi SK, Chien S, Bayat S and Bayat M: Improvement in infected wound healing in type 1 diabetic rat by the synergistic effect of photobiomodulation therapy and conditioned medium. J Cell Biochem 120: 9906-9916, 2019.
25. Guo J, Hu Z, Yan F, Lei S, Li T, Li X, Xu C, Sun B, Pan C and Chen L: Angelica dahurica promoted angiogenesis and accelerated wound healing in db/db mice via the HIF-1α/PDGF-β signaling pathway. Free Radic Biol Med 160: 447-457, 2020.
26. Jiang W, Zhang J, Zhang X, Fan C and Huang J: VAP-PLGA microspheres (VAP-PLGA) promote adipose-derived stem cells (ADSCs)-induced wound healing in chronic skin ulcers in mice via PI3K/Akt/HIF-1α pathway. Bioengineered 12: 10264-10284, 2021.
27. Liu W, Yuan Y and Liu D: Extracellular vesicles from adipose-derived stem cells promote diabetic wound healing via the PI3K-AKT-mTOR-HIF-1α signaling pathway. Tissue Eng Regen Med 18: 1035-1044, 2021.

28. Veith AP, Henderson K, Spencer A, Sligar AD and Baker AB: Therapeutic strategies for enhancing angiogenesis in wound healing. Adv Drug Deliv Rev 146: 97-125, 2019.
29. Aoki M and Fujishita T: Oncogenic roles of the PI3K/AKT/mTOR axis. Curr Top Microbiol Immunol 407: 153-189, 2017.
30. Han J, Huang C, Jiang J and Jiang D: Activation of autophagy during farnesyl pyrophosphate synthase inhibition is mediated through PI3K/AKT/mTOR signaling. J Int Med Res 48: 300060519875371, 2020.
31. Rai SN, Dilnashin H, Birla H, Singh SS, Zahra W, Rathore AS, Singh BK and Singh SP: The role of PI3K/Akt and ERK in neurodegenerative disorders. Neurotox Res 35: 775-795, 2019.
32. Zubair M and Ahmad J: Role of growth factors and cytokines in diabetic foot ulcer healing: A detailed review. Rev Endocr Metab Disord 20: 207-217, 2019.
33. Zhu Y, Wang Y, Jia Y, Xu J and Chai Y: Roxadustat promotes angiogenesis through HIF-1α/VEGF/VEGFR2 signaling and accelerates cutaneous wound healing in diabetic rats. Wound Repair Regen 27: 324-334, 2019.
34. Hart PH and Norval M: Ultraviolet radiation-induced immunosuppression and its relevance for skin carcinogenesis. Photochem Photobiol Sci 17: 1872-1884, 2018.
35. Amin KN, Umapathy D, Anandharaj A, Ravichandran J, Sasikumar CS, Chandra SKR, Kesavan R and Mohanram RK: miR-23c regulates wound healing by targeting stromal cell-derived factor-1α (SDF-1α/CXCL12) among patients with diabetic foot ulcer. Microvas Res 127: 103924, 2020.
36. Wang Y, Zhu J, Chen J, Xu R, Groth T, Wan H and Zhou G: The signaling pathways induced by exosomes in promoting diabetic wound healing: A mini-review. Curr Issues Mol Biol 44: 4960-4976, 2022.